Visualization and research of gas-liquid two phase flow structures in cylindrical channel

Sebastian Stefański[1*], *Wojciech* Kalawa[1], *Kaja* Mirek[1] and *Maciej* Stępień[1]

[1] AGH University of Science and Technology, Faculty of Energy and Fuels, Department of Thermal and Fluid Flow Machines, al. Mickiewicza 30, 30-059 Krakow

Abstract. Two-phase flows are commonly found in many industries, especially in systems, where efficient and correct functioning depend on specific values of flow parameters. In thermal engineering and chemical technology the most popular types of two-phase mixture are gas-liquid or liquid-vapour mixtures. Bubbles can create in flow different structures and determine diverse properties of flow (velocity of phase, void fraction, fluctuations of pressure, pipe vibrations, etc.). That type of flow is difficult to observe, especially in liquid-vapour mixture, where vapour is being made by heating the medium. Production of vapour and nucleation process are very complicated issues, which are important part of two-phase flow phenomenon. Gas-liquid flow structures were observed and described with figures, but type of structure depends on many parameters. Authors of this paper made an attempt to simulate gas-liquid flow with air and water. In the paper there was presented specific test stand built to observe two-phase flow structures, methodology of experiment and conditions which were maintained during observation. The paper presents also the structures which were observed and the analysis of results with reference to theoretical models and diagrams available in literature.

1 Introduction

Two-phase flows are commonly found in many industries, especially in systems, where efficiency is determined by specific parameters of mixture flow. In thermal and chemical engineering the most popular types of two-phase flows are gas-liquid and liquid-vapour mixtures. In heat and power engineering two phase flows can be found in boiler pipes producing steam and in evaporators of refrigerating systems. Structure of two-phase flow has an important impact on heat and mass transfer, so it is important to observe and specify characteristics of structures. Productions of vapour and nucleation process are very complicated issues, which are important part of two-phase flow phenomenon. Gas-liquid flow structures were observed and described with figures, but type of structure depend on many parameters, such as diameter of the pipe, volume flow rate of each phase, void fraction and heat flow value [1].

* Corresponding author: stefanski@agh.edu.pl

2 Fundamentals

Two-phase flow structures are determined by position (angle) of pipe and flow direction of the mixture (upwards or downwards). For vertical orientation and upwards flow structures from figure 1 can be observed. In case of downwards flows the observed structures are different. There is a lack of a common opinion about their systematics in the literature. The exemplary classification is given below, in the figure 2.

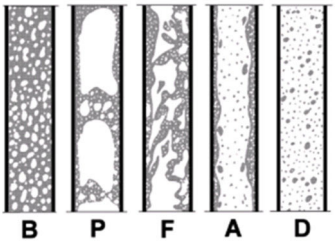

Fig. 1. Two-phase flow structures for vertically oriented channel (upwards flow) [2]

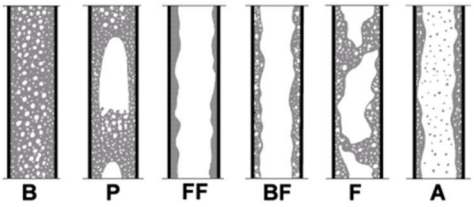

Fig. 2. Two-phase flow structures for vertically situated channel (downwards flow) [2].
B –bubble flow, P – plug flow, F – floating film flow, BF – bubble-foam flow, F – foam flow, A – annular flow

The structures presented in figure 1 are described as follows:
- bubble flow (B) – gas phase constitute dispersed bubbles in continuous liquid phase, with similar velocity;
- plug flow (P) – gas phase constitute plugs occupies almost the whole diameter of the channel;
- foam flow (F) – continuity of liquid phase is disturbed by high volume flow of gas phase;
- annular flow (A) – liquid phase flows on inner surface of the channel with high velocity of gas phase in the middle;
- dispersed flow (D) – high volumetric flow rate of the gas phase causes formation of small drops of liquid [2].

Due to the fact that the boundary between structures is difficult to observe, it is common to apply simpler classification including below mentioned structures:
- bubble flow (B),
- transitory flows (P, F),
- annular flows (A, BF, FF).

Radically different structures can be observed in horizontally situated channels. The classification of two-phase flow structures suggested by Baker is presented in the figure 3 [2].

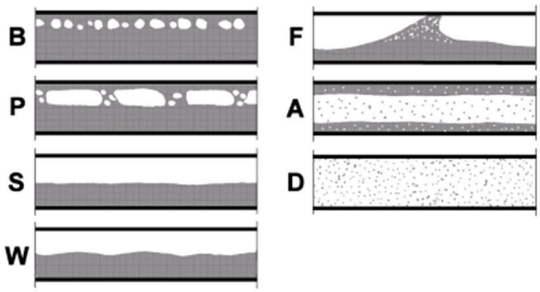

Fig. 3. Two-phase flow structures for horizontally oriented channel [2].

The structures presented in the figure above are defined as:

- bubble flow (B) – in the continuous liquid phase there are bubbles cumulating in the upper part of the channel;
- plug flow (P) – gas phase flows in continuous liquid phase in round shape plugs cumulated in upper part of a channel;
- stratified flow (S) – continuous gas phase flows in the upper part of the channel, phases separation surface is smooth;
- wavy flow (W) – the structure which is formed as a result of volumetric flow rates increase;
- flash flow (F) – phases separation surface is wavy and wave picks touches upper wall of the channel;
- annular flow (A) – liquid phase constitute thin layer on the inner channel surface, gas phase flows in the middle of the pipe, asymmetry of the liquid layer thickness there may occur and the surface between phases is wavy;
- disperse flow (D) – the structure found when the gas phase velocity is significantly higher than liquid, drops are entrained from wave picks; for extreme conditions liquid layer fades and the whole medium flows as small drops [2].

Extent of structure occurrence can be presented on chart known as regime map depending on particular parameters, where structures are represented by areas separated with lines (fig. 4). The regime maps can be based on different coordinate systems, channel geometry and the direction of mixture flow. Usually on the axes can be values of velocities, volumetric flow rates, mass flow rates or phases' physical properties such as viscosity, density, surface tension. Lines separating the areas of structures cannot be considered as the strict boundary of two phenomena. It is the result of the complexity of two-phase flow issue reflected in combining two different types of flow structure [3].

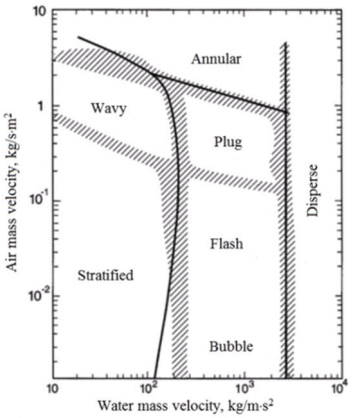

Fig. 4. Weisman chart. The regime map of air-water mixture flow in cylindrical channel (int. diameter 51mm) depending on air and water mass flow rates [3].

3 Methodology of experiment

3.1 Test stand

Two-phase flow structures were observed using the test stand consisting of several autonomic parts (fig. 5, 6). The basic element of this stand is pumping system including impeller pump (10), suction and delivery pipelines with flow regulation valve (1), pressure transducer (2),

water temperature sensor (3), flowmeter (4). Pump operation parameters and pipelines diameters determined technical characteristics of farther part of the stand. Pumping system was equipped with control unit which enables to control volumetric flow rate of water and display values from sensors. Cylindrical channel used for observations of two-phase flow structures is made of acrylic, an 1800 mm long pipe with internal diameter 56 mm (7). The pipe was permanently connected to steel mountings. This element was connected to steel rack using flange coupling. To the flanges there are connected normalized hydraulic pipes and hoses. In the flange installed on the delivery pipeline there were two 5 mm channels used for supply air to transparent channel (5, 6).

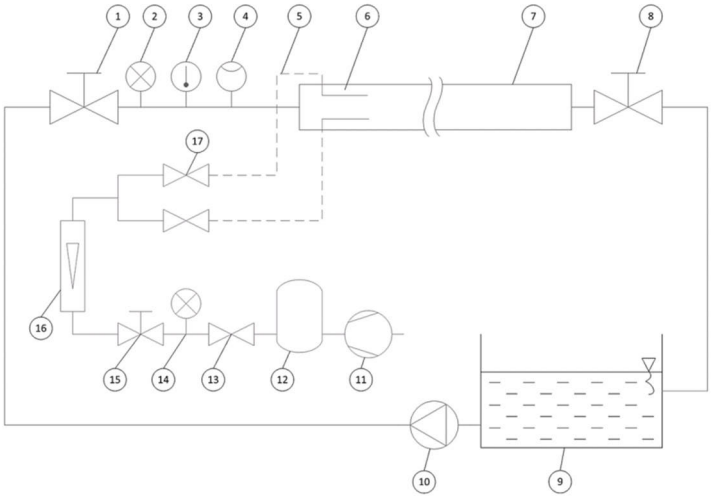

Fig. 5. Test stand diagram. 1 – flow regulation valve, 2 – pressure transmitter, 3 – thermometer, 4 – flowmeter, 5 – air flexible hose, 6 – air supply system, 7 – acrylic channel, 8 – pressure regulation valve, 9 – opened water container, 10 – circulation pump, 11 – compressor, 12 – gas cylinder, 13 – pressure regulation valve, 14 – manometer, 15 – flow regulation valve, 16 – rotameter, 17 – valve

The aim of the project was to build a compact test stand which enables observing two-phase flow structures in the horizontally and vertically oriented pipe with downwards and upwards direction of flow. For this reason the steel rack is connected to basic frame with bolt. That connection allows changing the angle between the transparent channel and ground.

Water is pumped (10) to the flow regulation valve (1) and then it flows through the pressure transducer (2), temperature sensor (3), and flowmeter (4). With the flexible hose water is directed to transparent acrylic channel (7). Behind the channel there is the DN65 valve (8) used for controlling the mixture pressure. With the second flexible hose water is directed to the opened container (9) where the phases of mixture are separated. From that container water transported to the suction port of the pump. The other phase in the mixture is air supplied with the compressor (11) to the gas cylinder (12). Pressure of air can be regulated with the valve (13). Compressed air flows through the flexible 8mm air hose to the manometer (14), flow regulation valve (15), rotameter (16) and then to T-pipe splitting the flow between two ports in flange connected to the channel. Air flow in each port can be regulated with the valves (17) installed on flexible hoses (5). The air is distributed to the transparent channel with two 10 cm long hoses with a diameter 6 mm (6).

Two-phase flow structures are observed with high speed video camera (300 FPS) (5, fig. 6) and graphically edited with computer software. For better lightning of the channel there is LED band installed on steel rack under the channel, and the matt screen placed behind the channel (fig. 7).

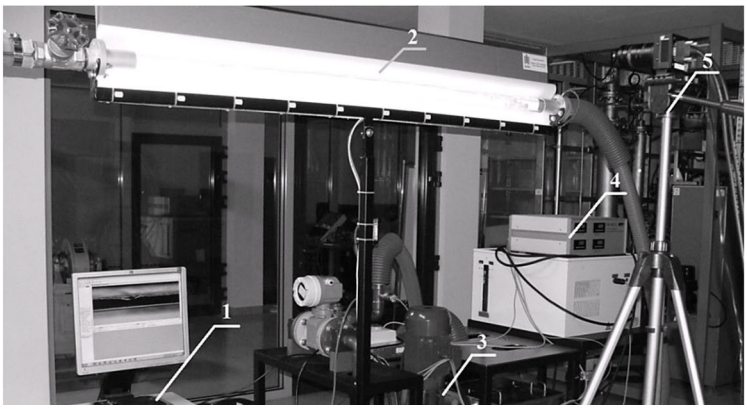

Fig. 6. Photo of test stand. 1 – data canvassing station, 2 – acrylic channel, 3 – pumping system, 4 – control unit, 5 – high speed video camera

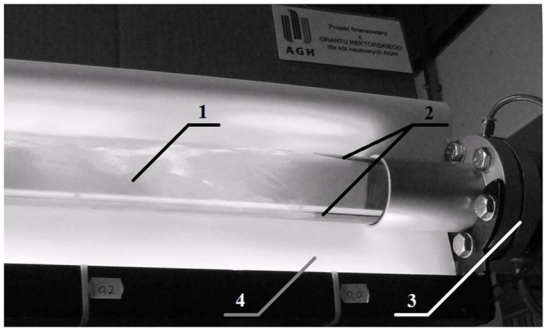

Fig. 7. Photo of inlet of acrylic channel and air supply system. 1 - acrylic pipe, 2 - air supply hoses, 3 - flange coupling, 4 - screen

3.2 Experiment procedure

For the purpose of making the analysis of the results easier and enabling the reference to studies available in literature, there were recreated conditions similar to the air-water flow structures studies by Weismann [3] (horizontal and vertical downwards direction of the flow) and Barnea [4] (vertical upwards direction of the flow). The geometry of pipe applied in those studies (int. diameter 51 mm) was the most similar to acrylic channel in authors' test stand (int. diameter 56 mm). Conditions set in Weismann's and Barnea's experiments were following: net pressure of the mixture 1 bar, temperature 25°C. To achieve similar conditions of experiment, air was being supplied with one orifice located in the inlet of the channel.

During the experiment two-phase flow structures in horizontal and vertical orientation were observed. For each configuration of the channel there was carried out series of measurements for volumetric air and water flows given in the table 1.

Table 1. Test point flow values.

Water volumetric flow rate, $\dot{V}_w,\ l/min$	10		30		100		200		400	
Air volumetric flow rate, $\dot{V}_a,\ l/min$	10	50	10	50	10	50	10	50	10	50

The test stand was set in particular configuration before each series of experiment. Water volumetric flow rate was set on value given in table 1 and after stabilization of flow parameters; air was supplied with the net pressure of 1 bar. When volumetric flow rate

fluctuations were less than 1 l/min, the net pressure of the mixture were set with the regulation valve on 1 bar. Observed structures were registered with high speed video camera on the length of 0.4 m. This procedure was repeated for each test point. Canvassed sequences of frames were subjected to graphic processing and compared to studies and diagrams available in literature.

4 Results of experiment

Tests taken according to described methodology enabled to observe and canvass two-phase flow structures for three stand configurations. The results of experiment, that is type of observed structure and volumetric flow rates of phases, are collected in table 2.

Table 2. The results of experiment for three configurations of test stand.

Direction of the flow	Vertical, downwards		Vertical, upwards		Horizontal	
Water volumetric flow rate [l/min]	Air volumetric flow rate [l/min]					
	10	50	10	50	10	50
10	Annular	Annular	Plug	Plug	Stratified	Stratified
30	Annular	Annular	Foam	Foam	Stratified	Wavy
100	Annular	Combined	Bubble	Foam	Flash	Wavy
200	Bubble	Bubble	Bubble	Bubble	Flash	Flash
400	Bubble	Bubble	Bubble	Bubble	Bubble	Bubble

For horizontally oriented channel structures of two-phase flow are radically different from the vertically ones. The reason of those differences is fact that buoyant and gravity force act perpendicularly to the direction of the flow. Structures which were observed for that configuration are consistent with theoretical classification [2]. They are presented in figure 8.

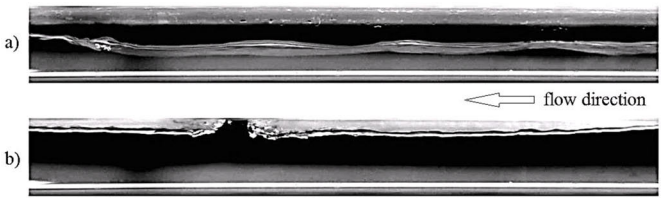

Fig. 8. Structures of two-phase flow for horizontally directed flow. a – wavy flow (water volumetric flow rate 30 l/min, air volumetric flow rate 50 l/min), b – flash flow (water volumetric flow rate 100 l/min, air volumetric flow rate 10 l/min). Flow direction from right to left.

Characteristic feature of downwards flow in vertical orientation is deceleration of air bubbles in relation to water velocity. It is caused by buoyant force acting on bubbles and oriented upwards. For considered range of test points there were two structures included in classification described by Oschinovo and Charles [5]. In the figure 9 there are presented photos of two structures which were observed during experiment. For upwards flow the buoyant force caused acceleration of the bubbles in relation to liquid phase velocity. For that reason the structures of flow presented above appear for different test points than for downwards flow configuration. Exemplary structures are presented in figure 10.

Fig. 9. Structures of two-phase flow for upwards flow. a – bubble flow (water volumetric flow rate 200 l/min, air volumetric flow rate 10 l/min), b – plug flow (water volumetric flow 10 l/min, air volumetric flow rate 10 l/min)

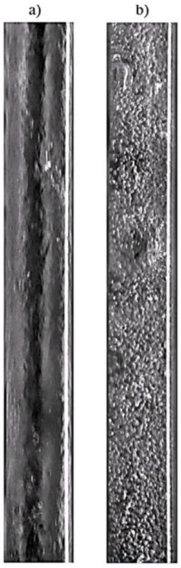

Fig. 10. Structures of two-phase flow for downwards flow. a – annular flow (water volumetric flow 30 l/min, air volumetric flow rate 10 l/min), b – bubbles flow (water volumetric flow rate 100 l/min, air volumetric flow rate 10 l/min)

4.1 Experimental uncertainties

For verification of the experiment results with regime maps, there is essential to calculate other parameters characterising two-phase flow, such as apparent velocities of phases and apparent mass velocities in flow.

The test stand was equipped with following measuring devices:

- pressure transmitter Huba Control 691 -1÷9 bar, max. measurement error 0.3% f.s.,
- RTD thermometer Endress+Hauser Omnigrad T TST487, max. measurement error ±0.25Ω (25°C),
- electromagnetic flowmeter Endress+Hauser Proline Promag 10W, max. measurement error ±0.5% o.r.,
- spiral pressure gauge -1÷10 bar, max. measurement error ±0.2 bar,
- rotameter Dwyer MMA 5÷50 l/min, max. measurement error 4% f.s.

On the basis of measurement errors of apparatus the calculation of apparent velocities and mass velocities measurement uncertainties were carried out. For that calculation best-worst case analysis were used. Values of air flow rate read from rotameter were calculated for each test point because of nonstandard operating conditions as follows:

$$\dot{V}_a = \dot{V}_{ar} \cdot \sqrt{\frac{p \cdot T_N}{p_N \cdot T}} \tag{1}$$

where:

$\dot{V}_a$ - standard air flow rate corrected for pressure and temperature
$\dot{V}_{ar}$ - actual air flow rate reading
p - actual absolute air pressure, bar
T_N - normal temperature NTP, 293.15 K

p_N - normal pressure NTP, 1 bar
T - actual air temperature, K

For temperature of air T=(25±1)°C and pressure p_a=(1±0.2) bar there was estimated air density ρ_a=(2.34±0.24) kg/m^3 on the basis of ideal gas law [6]. Density of water was estimated to be (997.1±0.1) kg/m^3 [6]. The next step was calculation of apparent velocities of phases.

The apparent velocity is defined as the linear velocity on the assumption that the whole volumetric flow rate passes through full cross-section area of the channel. It can be calculated using formula (2) [7].

$$u_i = \frac{\dot{V}_i}{A} \tag{2}$$

where:
u_i - apparent velocity of phase *i,* m/s
$\dot{V}_i$ - volumetric flow rate of phase *i*, m^3/s
A - channel cross-section area, 24.64 ·10^{-4} m^2

Apparent velocities uncertainties were estimated with best-worst case analysis using flow rate measurement error. The results are presented in table 3.

By analogy, apparent mass flow rate of the phase is defined as mass flow rate in relation to cross-section of the channel like in the formula (3) [7] given below.

$$w_i = \frac{\dot{m}_i}{A} = \frac{\rho_i \cdot \dot{V}_i}{A} = \rho_i \cdot u_i \tag{3}$$

where:
w_i - apparent mass velocity of phase *i*, kg/(s·m^2)
$\dot{m}_i$ - mass flow rate of phase *i*, kg/(s·m^2)
ρ_i - density of phase *i*, m^3/kg
A - cross-section area, m^2
u_i - apparent velocity of phase *i*, m/s

Apparent mass velocities uncertainties were estimated by analogy to previous analyses, using flow rate measurement error and density uncertainties. The results are presented in table 4.

Table 3. Apparent velocities and mass velocities of phases in channel for different flow rates.

Water volumetric flow rate, $\dot{V}_w, \frac{l}{min}$	10	30	100	200	400
Water volumetric flow rate, $\dot{V}_w, \frac{dm^3}{s}$	0.167 ±0.001	0.500 ±0.003	1.667 ±0.008	3.333 ±0.017	6.667 ±0.033
Apparent water velocity, $u_w, \frac{m}{s}$	**0.0677 ±0.000 3**	**0.2030 ±0.001 0**	**0.6767 ±0.003 4**	**1.3534 ±0.006 8**	**2.7070 ±0.013 5**
Apparent mass water velocity, $w_w, \frac{kg}{s \cdot m^2}$	**68 ±1**	**202 ±1**	**675 ±3**	**1349 ±7**	**2699 ±14**

Air volumetric flow rate, $\dot{V}_a, \frac{l}{min}$	10	50
Air volumetric flow rate, $\dot{V}_a, \frac{dm^3}{s}$	0.167 ±0.033	0.833 ±0.033
Apparent air velocity, $u_a, \frac{m}{s}$	**0.0677 ±0.0135**	**0.3383 ±0.0135**
Apparent mass air velocity, $w_a, \frac{kg}{s \cdot m^2}$	**0.158 ±0.048**	**0.792 ±0.113**

The calculations described with formulas (1) and (2) enabled to give results on regime maps available in literature [3] [4]. The results of experiment given on the abovementioned regime maps are presented in the figures 11-13 below.

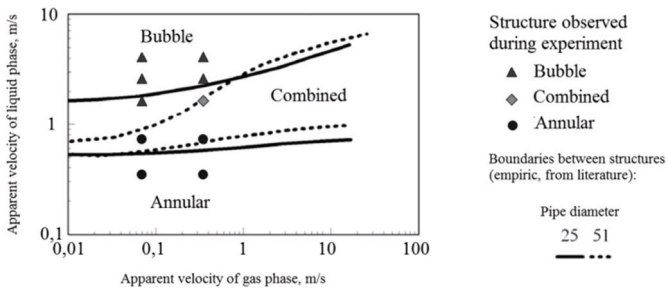

Fig. 11. Experimental results in comparison to Barnea's regime map [4] for downwards vertical gas-liquid flow in pipes with diameter of 25 mm and 51 mm, net pressure 0,1 MPa and temperature of the mixture 25°C.

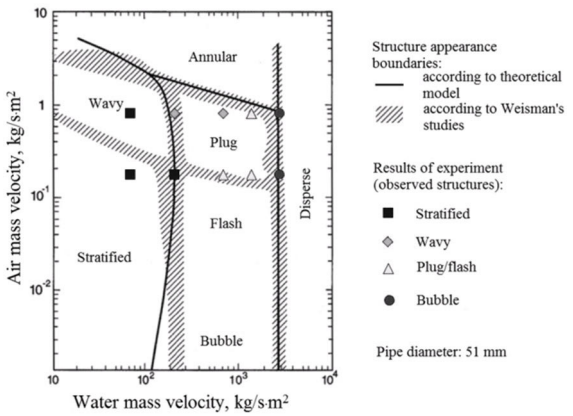

Fig. 12. Experimental results in comparison to Weisman's regime map [3] for horizontally directed gas-liquid flow in pipe with diameter of 51 mm, net pressure 0,1 MPa and temperature of mixture 25°C.

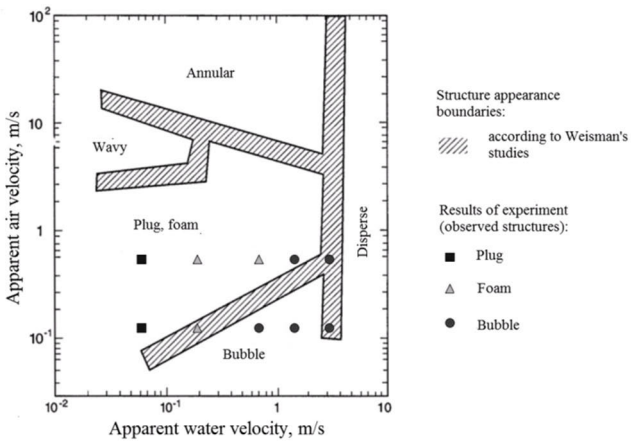

Fig. 13. Experimental results in comparison to Weisman's regime map [3] for upwards vertical gas-liquid flow in pipe with diameter of 25 mm, net pressure 0,1 MPa and temperature of mixture 25°C.

5 Conclusions

Comparing the experimental results to regime maps developed for geometrically similar systems working under close net pressure lead to the conclusion that the test stand correctly fulfills its role. A great majority of observed two-phase flow structures can be adjusted to the areas from literature regime maps. Slight deviations from empirically developed areas in regime maps are caused by gradual change of the structure when changing the parameters of the flow and geometry of considered channel. The boundaries defined on the maps describe the probability of changing from one structure to the other, not the exact conditions for its appearance [1]. The performed tests proved that there is possibility of existence of different two-phase flow structures and strong differences in interfacial turbulence. Disturbances in the two-phase flow in industrial systems have direct influence on heat transfer coefficient value, which determine the intensity of heat transfer, for example during boiling process.

Making the comparison of results obtained in experiment to those found in literature shows that the published regime maps cannot be taken as universal ones. Possibility of appearance of the particular structure is determined by many parameters, for instance temperature, net pressure, geometry of the channel and thermodynamic characteristic of fluids. For that reason adjusting the map for comparing one experiment to the other must consider the compatibility of mentioned parameters.

Test stand does not enable achieving as high phases velocities as presented on regime maps available in literature. It is cause by volumetric flow rate limit of pump and compressor installed in the test stand. Disperse flow could not be observed during the experiment for any flow direction. Despite described limits and problems, the test stand provides scientific and didactic value, and with some improvements can be used for further analysis or observations.

References

1. A. Kuchczyńska, *Warunki pracy aparatu ze wznoszącym i opadającym przepływem dwufazowym gaz-ciecz*, doctor's thesis, Opole (2010)
2. Didactic materials for subject *Operacje Mechaniczne w Inżynierii Procesowej*, Opole University of Technology (2015)
3. J. Weisman, *Two-Phase Flow Patterns. Handbook of Fluids in Motion*, Ann Arbor Science Publ., (1983)
4. D. Barnea, *A unified model for predicting flow-pattern transitions for the whole range of pipe inclinations*, International Journal of Multiphase Flow (1987)
5. R. Koch, A. Noworyta, *Procesy mechaniczne w inżynierii chemicznej*, WNT (1992)
6. K. Ražnjević, *Handbook of Thermodynamic Tables and Charts,* Hemisphere Publishing Corporation (1976)
7. Z. Orzechowski, *Mechanika płynów w inżynierii środowiska*, WNT (1997)